

SAX_SR_2002
Revision: 1.0
September 30, 2002



HTG - Hyperschall Technologie Göttingen
Max-Planck-Str. 19
37191 Katlenburg-Lindau
Germany

BeppoSAX Re-entry Analysis with SCARAB

HTG-Report-02-8

Summary Report

Destructive Re-Entry Analysis of BeppoSAX with SCARAB

Prepared by:
Tobias Lips

DOCUMENT STATUS SHEET

DOCUMENT TITLE: BeppoSAX Re-entry Analysis with SCARAB			
DOCUMENT REFERENCE NUMBER: SAX_SR_2002			
ISSUE:	REVISION:	DATE:	REASON FOR CHANGE:
Draft	0.1	September 18, 2002	Initial version
Draft	0.9	September 27, 2002	Internal Review
Final	1.0	September 30, 2002	Final version after internal review

SIGNATURES AND APPROVALS:			
	DATE:	NAME:	SIGNATURE (on original):
Prepared	September 27, 2002	T. Lips	
Checked	September 27, 2002	B. Fritsche	
Approved	September 30, 2002	T. Lips	
Authorized	September 30, 2002	G. Koppenwallner	



TABLE OF CONTENTS

Document Status Sheet.....	2
Table of Contents	3
1 Introduction	4
1.1 BeppoSAX	4
1.2 SCARAB Software System.....	5
2 BeppoSAX Modelling with SCARAB.....	7
2.1 Geometry and Mass Model	7
2.2 Structural Model.....	9
2.3 Tank Model	10
2.4 Summary	12
3 BeppoSAX Re-entry Analysis with SCARAB	13
3.1 Initial Conditions.....	13
3.2 Re-entry and Fragmentation History.....	13
3.3 Ground Impact Fragments.....	20
3.4 Casualty Area	26
4 Summary	29
References	30

1 INTRODUCTION

1.1 BeppoSAX

The X-ray astronomy satellite BeppoSAX (Satellite per Astronomia X, "Beppo" in honor of Giuseppe Occhialini), is a project of the Italian Space Agency (ASI) with participation of the Netherlands Agency for Aerospace Programs (NIVR). BeppoSAX was launched by an Atlas G-Centaur directly into a circular 600 km orbit at 3.9 degrees inclination on April 30, 1996. The satellite is a three axis stabilized spacecraft with a total mass of about 1400 kg. The main dimensions in flight configuration are about 2450 mm x 8980 mm x 3650 mm.

Figure 1-1 shows the origin and the orientation of the main coordinate system of the satellite. The pictures of the satellite are already images generated by SCARAB based on the complete satellite model.

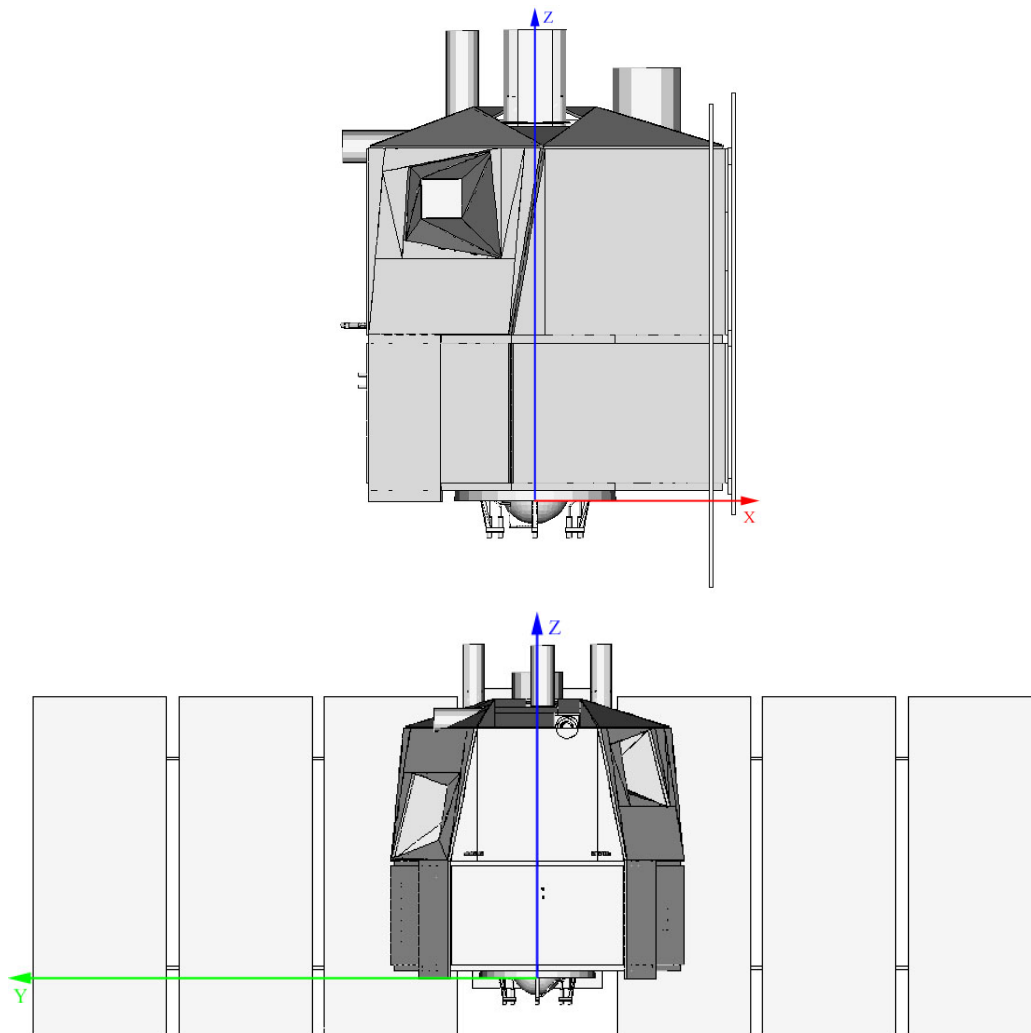


Figure 1-1: Coordinate System of BeppoSAX

Current (September 25, 2002, 10:06 UTC) orbit status:

- Semi major axis: $a = 6811.9244 \text{ km}$
- Eccentricity: $\varepsilon = 0.000507$
- Inclination: $i = 3,96271^\circ$
- Right ascension of the ascending node: $\Omega = 324,838977^\circ$
- Argument of perigee: $\omega = 169,739011^\circ$
- True anomaly: $\varphi = 190,244766^\circ$

The current flight altitude is about 433.8 km. Figure 1-2 compares the development of the flight altitude of BeppoSAX and the German X-ray telescope satellite ROSAT. It also shows the propagated development provided by ASI and HTG.

The first propagation of HTG was based on the orbital data of BeppoSAX in June 2002 and obviously a too pessimistic prediction for the solar activity. The second one is based on the current data and recent predictions for the solar activity.

Therefore, HTG now predicts the re-entry for the end of 2003.

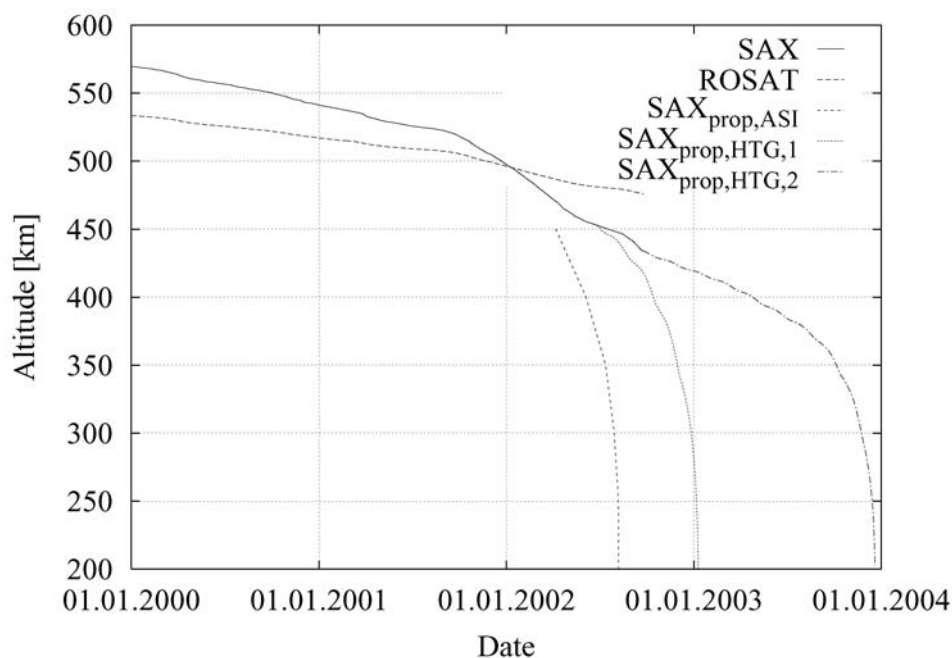


Figure 1-2: Flight altitude of BeppoSAX and ROSAT

Due to the relatively high mass of BeppoSAX it has to be expected that parts of the satellite will survive the re-entry into the earth atmosphere. With the later on described software tool SCARAB the destruction of a spacecraft during re-entry can be calculated in order to determine how much of it and how many parts will reach the ground.

1.2 SCARAB Software System

The SCARAB software system (SpaceCraft Atmospheric Re-Entry and Aerothermal Break-Up) has been developed during the last 6 years within the frame of several ESOC contracts. During the last two years the SCARAB software has been tested against the NASA ORSAT code and, in addition, applied to several projects, namely an ATV re-entry analysis, a ROSAT



re-entry analysis and an Ariane-5 re-entry. The practical application of SCARAB to project work has been demonstrated. SCARAB is on the way to become the European standard software for re-entry destruction analysis.

Currently SCARAB version 1.5 is used at HTG. Version 2.0 is available but has not yet been tested in detail. The development of SCARAB 3.0 has just started in January 2002 and will be finished in 2005. SCARAB 3.0 is expected to be a releasable version which can be provided to the national space agencies of ESA member states.

The main capabilities of SCARAB are:

1 Spacecraft Modeling

This module allows modeling the re-entry object with all important properties, namely:

- Detailed geometry module with panel generation
- Extensive and individual expandable material database
- Automated generation of mass and thermo-physical model

2 External Loads on Spacecraft

This module calculates continuously the actual aerodynamic and aerothermal loads acting on the spacecraft. It considers every change in flight attitude and geometry.

3 Spacecraft Response

Several modules combine:

- 6D re-entry analysis
- 2D thermal analysis
- Structural analysis based on engineering cut methods

4 Fragmentation

Fragmentation treats the destruction by melting on panel level and mechanical break-up of cuts. Fragments and subfragments are generated and calculated separately. Subfragments respectively final fragments are tracked down to the ground.

2 BEPPOSAX MODELLING WITH SCARAB

SCARAB (Version 1.5), a software system developed by Hyperschall Technologie Göttingen (HTG) for the European Space Operation Center (ESOC), has been used to model the satellite [1] and also later to perform the re-entry analysis [2]. SCARAB is a multidisciplinary tool which allows modeling a re-entry object with all its important properties: detailed panelized geometry, extensive material database, mass, thermo-physical, and structural model [3], [4].

2.1 Geometry and Mass Model

The geometry of BeppoSAX has been modeled as close to reality as possible. Due to the very detailed documentation provided by the satellite manufacturer this was possible down to component level of each subsystem. If possible or specified all parts have been modeled with the actual wall thickness. Otherwise the wall thickness was adapted to the mass of the part (specified in the mass budget). In particular, all the electronic boxes have been modeled in this way: boxes with the real outer dimensions but with a constant wall thickness matching the mass of the electronic box.

The satellite has been modeled with the following drawings and documents delivered by ALENIA:

- SAX Satellite Mass Budget Report (SX-RP-AI-003), Issue 12, 30/06/94, [7]
- SAX System Design Report (SX-RP-AI-118), Issue 01, 10/01/94, [8]
- Mass Properties Status Report Structure (SX-RP-AI-0031), Issue 06, 19/07/94, [9]
- ~140 large scale drawings (SX-IC-AI-006)

The satellite has been modeled in flight configuration with a full reaction control system (RCS) tank. This corresponds to the present configuration of the satellite in orbit.

The modeling followed the S/C hierarchy levels. Each subsystem (S/C and scientific payload subsystems) has been modeled very detailed with high accuracy.

The complete model consists of 859 “primitives” (basic geometric elements like spheres, boxes, circles, rectangles, triangles, cylinders, cones; see Figure 2-1).

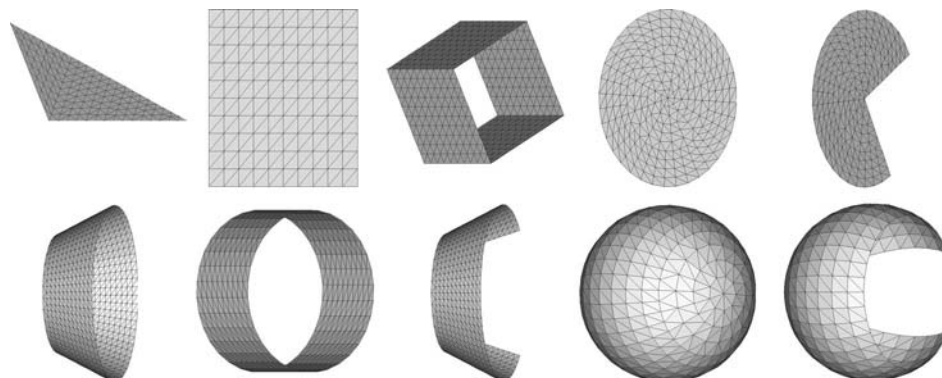


Figure 2-1: Set of Primitives in SCARAB

The geometric information of these primitives has been translated into a panelized model with 72,584 volume panels. In a last step each volume panel is transformed into surface panels. This yields 177,708 surface panels.

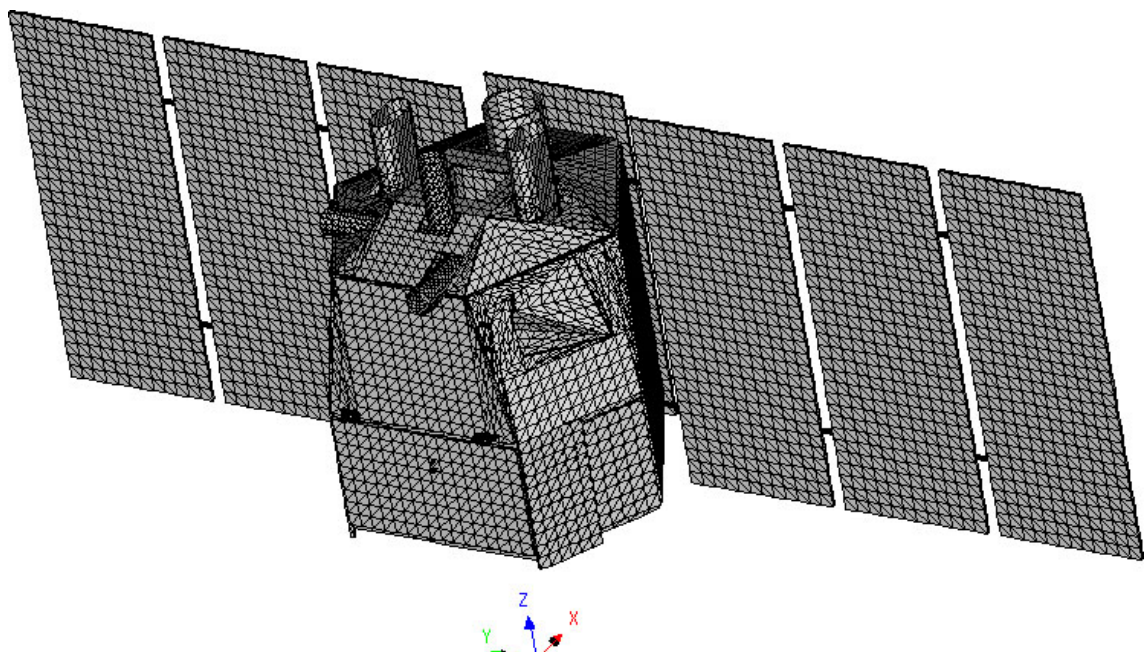
MODEL DATA					
Primitives	859	Volume Panels	72,584	Surface Panels	177,708
Materials	HC-AA5052 (s = 20, 30, 50 mm), HC-AA5052-C (s = 20, 30 mm), AA7075, AA2024, A316, Copper, Inconel718, Hydrazine (N2H4), Helium, Invar, TiAl6V4, CFRP				
MASS DATA					
Sub Components	Real Mass [kg]	Model Mass[kg]	Diff. [kg]	Diff. [%]	
STS	245.81	232.869	-12.941	-5.26	
TCS	71.16	63.564	-7.596	-10.67	
EPS	144.22	144.481	0.261	0.18	
ODBH	56.46	56.487	0.027	0.05	
TT&C	10.61	9.464	-1.146	-10.80	
RCS	48.56	40.988	-7.572	-15.59	
AOCS	97.1	97.317	0.217	0.22	
BMSP	9.32	12.466	3.146	33.76	
SAS	76.09	78.776	2.686	3.53	
HP-GSPC	109.66	109.714	0.054	0.05	
PDS	182.01	181.992	-0.018	-0.01	
WFC	94.49	95.014	0.524	0.55	
LECS	30.64	30.792	0.152	0.50	
MECS	82.92	82.685	-0.235	-0.28	
Harness	110.984	111.005	0.021	0.02	
Balance (Dummy) Masses	-	37.805	-	-	
TOTAL	1385.63	1385.419	-0.211	-0.02	
CENTER OF GRAVITY					
X [m]	0.001458	Y [m]	0.011921	Z [m]	1.125339
MOMENTS OF INERTIA					
I _{xx} [kg m ²]	1683.2950	I _{yy} [kg m ²]	1229.7803	I _{zz} [kg m ²]	1497.5246
I _{xy} [kg m ²]	-15.41467	I _{yz} [kg m ²]	-17.14787	I _{xz} [kg m ²]	68.418411
FIGURE					
					

Table 2-1: Complete Satellite

2.2 Structural Model

The structural analysis of SCARAB bases on an engineering cut model. Cut planes have to be defined. The primitives located within this cut plane are defined as joints. The joints are the load bearing parts. The structural module will calculate the actual stress and the breaking stress in these joints during the re-entry calculation.

The structural model consists of 6 “cuts” in order to analyze the stress in the hinges between each solar panel. The six cut planes are all parallel to the x-z-plane and located at the positions of the hinges between each solar panel (see Figure 2-2 and Table 2-2).

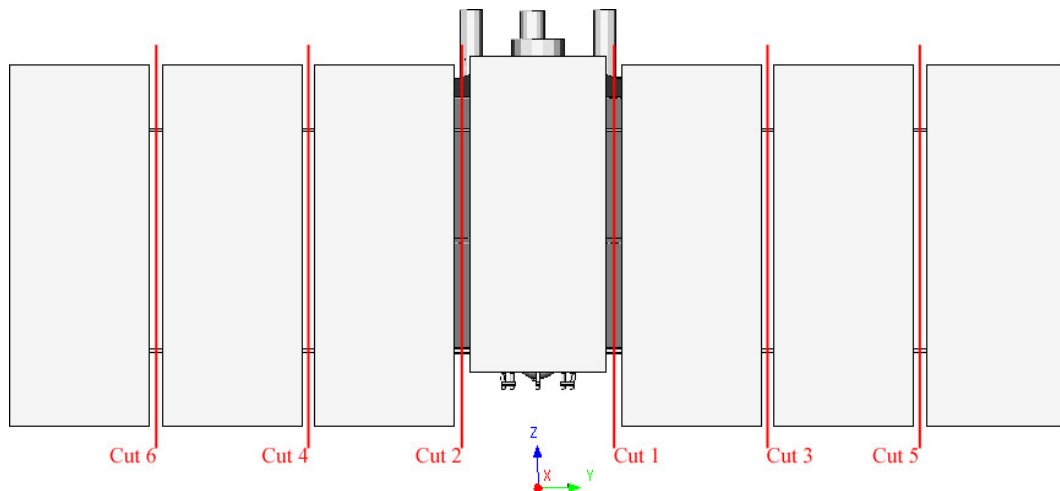


Figure 2-2: BeppoSAX Cut Model

CUT PLANE POSITIONS	
Cut No.	Y-Position [m]
1	0.655
2	-0.655
3	1.941
4	-1.941
5	3.227
6	-3.227

Table 2-2: Cut Plane Positions

The 12 joints have been modeled as massive rectangular connection elements made of A316. The dimensions of each joint are listed in Table 2-3.

JOINT DIMENSIONS			
Cut No.	X [mm]	Y [mm]	Z [mm]
1 – 2	22.8	132	25
3 - 6		106	

Table 2-3: Joint Dimensions

2.3 Tank Model

The tank of the RCS has been modeled including its liquid contents (26 kg hydrazine N_2H_4) in order to analyze tank bursting. The tank model input data are listed in Table 2-4.

TANK MODEL INPUT DATA	
Volume of the tank	44.8 l
Nominal burst pressure of the tank	68 bar
Material of the tank	TiAl6V4
Mass of the fluid tank content	26 kg
Type of fluid tank content	Hydrazine
Mass of the pressurisation gas	78.71 g
Type of pressurisation gas	Helium

Table 2-4: Tank Model Input Data

Most of these data were specified in the SAX System Design Report (SX-RP-AI-118) [8]. Only the mass of the pressurization gas has been calculated from the specified mean operation pressure (26 bar).

Figure 2-3 shows the results of the tank heating calculated with the SCARAB tank module. Assuming a uniform temperature distribution for both, the tank and the content, the bursting point is predicted to:

- Temperature: 472.93 K
- Pressure: 56.59 bar

This figure also shows that the fluid tank content will not evaporate because the tank pressure is always higher than the vapor pressure.

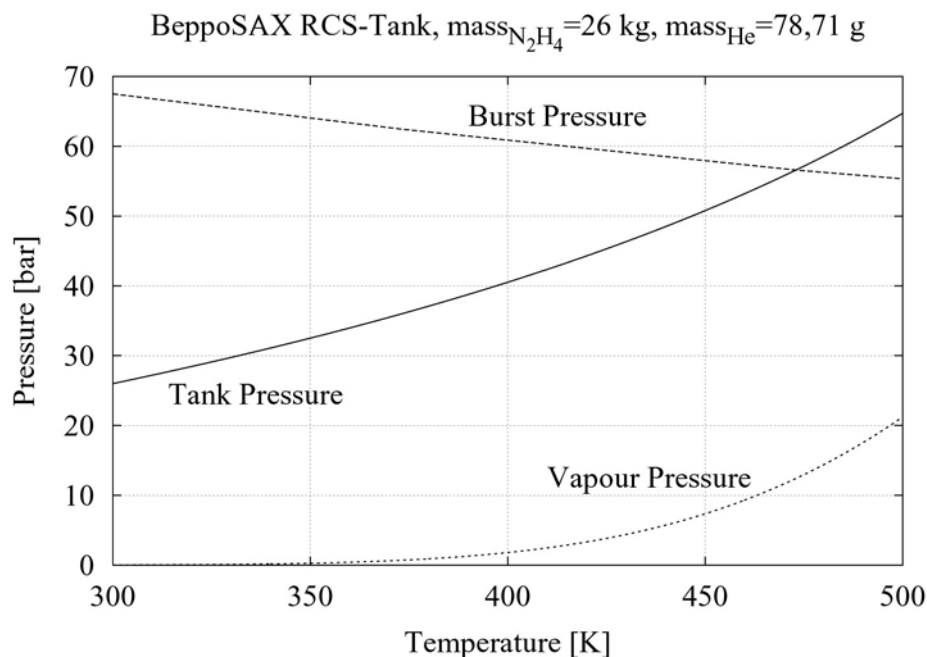


Figure 2-3: BeppoSAX RCS-Tank Heating (SCARAB Tank Module Results)

During the real re-entry calculation with SCARAB the assumption of a uniform temperature distribution would not be valid. It has to be expected that the tank shell will be heated much more than the content. This will happen because the tank shell is directly exposed to the flow and the content has a much higher thermal capacity (higher specific heat capacity and higher mass than the shell).

Figure 2-4 shows only the burst pressure of the RCS-Tank versus temperature.

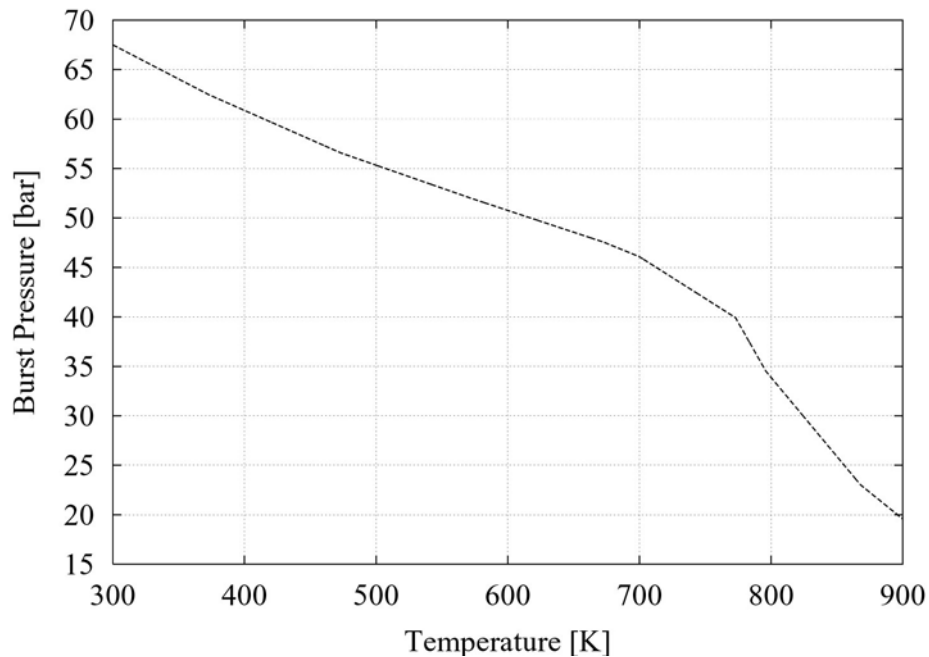


Figure 2-4: Burst Pressure of the RCS-Tank

2.4 Summary

A very high and accurate level of modeling has been achieved for BeppoSAX (see Table 2-5). Primarily, the total mass and the mass distribution of the model correspond almost completely to the data of the real satellite. The total model mass difference is below 0.02% (model mass: 1385.419 kg, real mass: 1385.63 kg). The center of gravity location of the complete BeppoSAX model matches the actual center of gravity within a distance below 12 mm. The modeled moments of inertia agree within the following bands: $I_{xx} < 3.3\%$, $I_{yy} < 0.9\%$, $I_{zz} < 5.8\%$.

MASS DATA				
	Real [kg]	SCARAB [kg]	Diff. [kg]	Diff. [%]
Total Mass	1385.63	1385.419	-0.211	-0.02
CENTER OF GRAVITY				
	Real [m]	SCARAB [m]	Diff. [mm]	Distance [mm]
X	0.001	0.001458	0.458	11.510
Y	0.010	0.011921	1.921	
Z	1.114	1.125339	11.339	
MOMENTS OF INERTIA				
	Real [kg m²]	SCARAB [kg m²]	Diff. [kg m²]	Diff. [%]
I _{xx}	1629.2	1683.2950	54.095	3.32
I _{yy}	1218.8	1229.7803	10.980	0.90
I _{zz}	1415.47	1497.5246	82.055	5.80
I _{xy}	-9.8	-15.41467	-5.615	-
I _{yz}	35.9	-17.14787	-53.048	-
I _{xz}	-8.6	68.418411	77.018	-

Table 2-5: Comparison of Model Data with Actual Data

3 BEPPOSAX RE-ENTRY ANALYSIS WITH SCARAB

3.1 Initial Conditions

In order to start a re-entry analysis the initial orbit and attitude conditions of the satellite have to be specified. The exact orbital parameters, right at the beginning of the re-entry, are yet unknown as well as the attitude and rotation of the satellite. Therefore they have been estimated based on the actual orbital status of BeppoSAX, or arbitrary chosen to reasonable values (see Table 3-1 and Table 3-2).

ACTUAL ORBIT PARAMETERS FOR BEPPOSAX	
June 26 2002, 7:06 UTC	
Semi major axis	6830.876 km
Eccentricity	0.000559
Inclination	3.961°
Right ascension of ascending node	315.448°
Argument of perigee	195.444°
True anomaly	164.590°

Table 3-1: Actual Orbit Parameters for BeppoSAX

ESTIMATED ORBIT PARAMETERS FOR BEPPOSAX	
January 2003	
Semi major axis	6500 km
Eccentricity	0.000559
Inclination	3.961°
Right ascension of ascending node	0°
Argument of perigee	0°
True anomaly	0°

Table 3-2: Estimated Orbit Parameters for BeppoSAX

The estimated initial data correspond to a geodetic altitude of 118.228 km, an aerodynamic velocity of 7.362 km/s, and a flight path angle of 0° (horizontal re-entry). The initial attitude conditions have been arbitrary set such that the x-axis of the satellite is aligned to the flight direction. The satellite does not rotate at the beginning of the re-entry.

3.2 Re-entry and Fragmentation History

During the re-entry the satellite fragmentizes very often. After each fragmentation two or more fragments are generated which have to be treated as separate re-entry objects. Generally, there is one main object (the heaviest fragment) and smaller sub-fragments. The main object is the most interesting because it will be the biggest fragment reaching the ground. In addition, the main object generates most of the sub-fragments, because sub-fragments mostly do not fragmentize again. They are relatively small and demise, or if they are big enough they reach ground.

In the following the results for the main object are presented as an example for the results for each fragment.

Figure 3-1 shows the altitude history of the main object. Until the velocity of a re-entry object becomes lower than Mach number 6 a full 6 degree of freedom integration of the equation of motion is performed. Below Mach number 6 a 3 degree of freedom analysis is conducted.

Figure 3-2 and Figure 3-3 show the histories of aerodynamic flight velocity and the flight path angle of the main object.

Figure 3-4 shows ground track of the main object in a map of the earth. The starting point of the re-entry calculation is on the equator in Indonesia (west of Borneo). The end point (impacting area) is in the Pacific Ocean (west of Colombia/Ecuador).

Figure 3-5 and Figure 3-6 illustrate the full 6D analysis because they show the history of angle of attack and slip angle for the main object. The main object rotates and oscillates mainly around the former y-axis of the satellite combined with an overlaid oscillation around the former z-axis (x-axis in flight direction corresponds to 0° angle of attack and 0° slip angle).

Figure 3-7 shows the maximum heat flux on the main fragment. The peak maximum heat flux is about 774 kW/m^2 at an altitude of 57.5 km (2067 s).

Figure 3-8 shows the maximum temperature of the main object. After 1563 s a constant temperature of 883 K is reached. This temperature corresponds to the melting temperature of the aluminum alloy AA5052. It takes about 135 s until the temperatures of other materials become higher. The overall peak maximum temperature is about 1723 K at an altitude of 65.9 km (2029 s).

The mass of the main object is shown in Figure 3-9. This figure illustrates that the melting starts 1667 s after the beginning of the calculation at an altitude of 99.1 km. Within 459 s the mass of the main fragments drops from 1341.485 kg down to 119.877 kg. This is not the total mass reaching the ground but only the mass of the biggest fragment. For the final masses of the other fragments see Table 3-4.

The presented and even more data have been calculated during the re-entry analysis. Together this yields 2.9 GB data. The complete analysis has taken about 3 weeks (~ 3 Pentium III processors at 1.2 GHz).

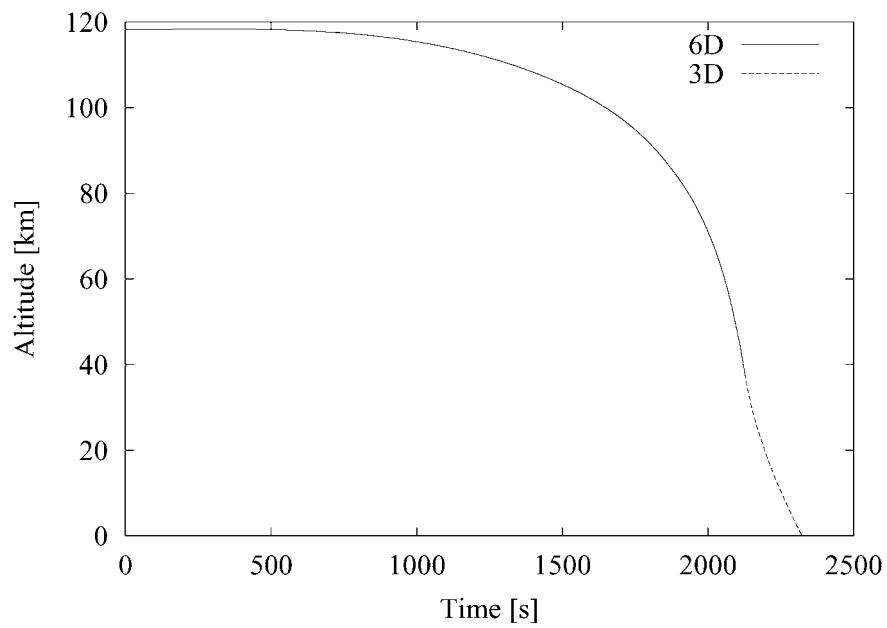


Figure 3-1: Altitude History of the Main Object

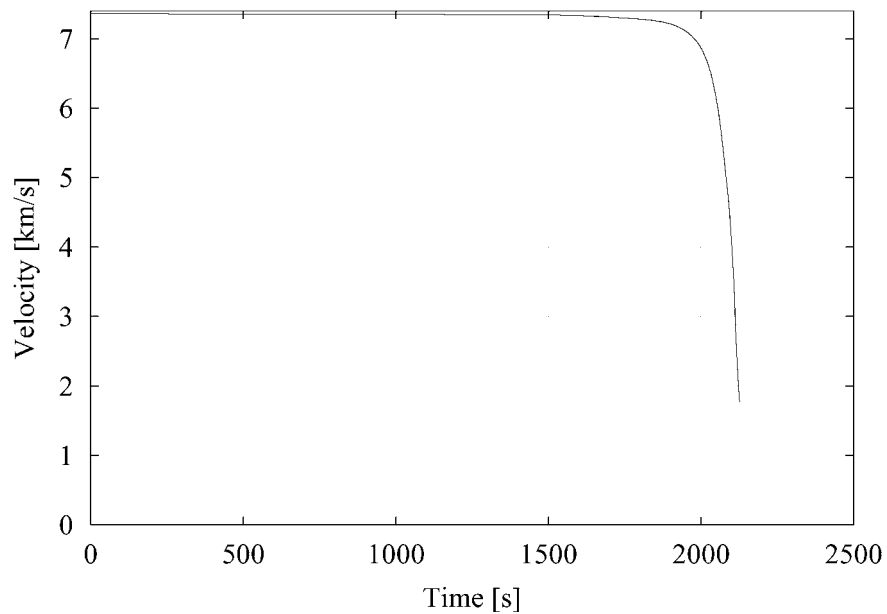


Figure 3-2: Velocity History of the Main Object

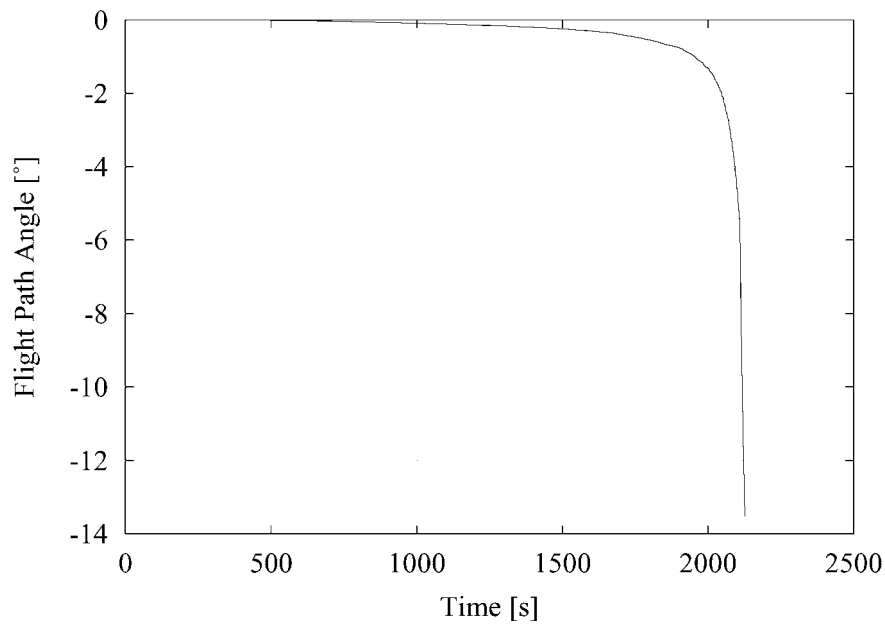


Figure 3-3: Flight Path Angle History of the Main Object

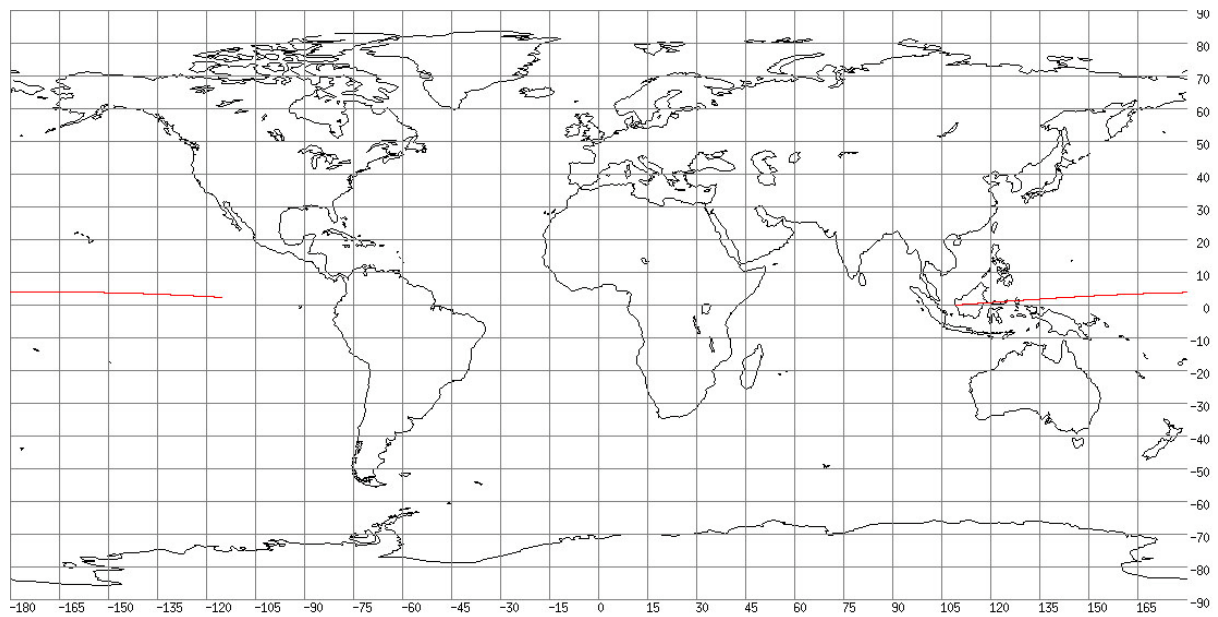


Figure 3-4: Ground Track of the Main Object

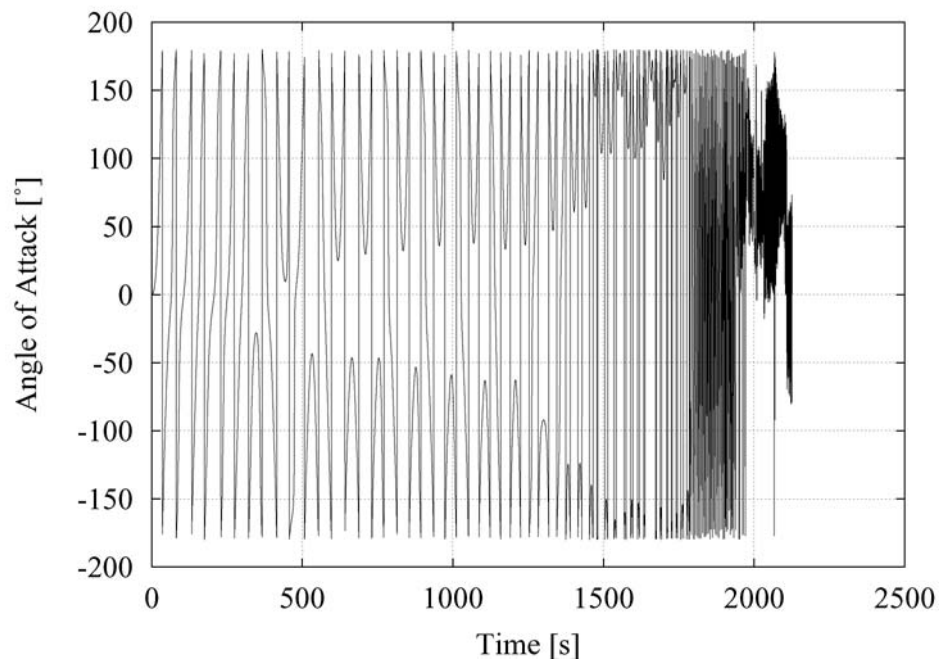


Figure 3-5: Angle of Attack History of the Main Object

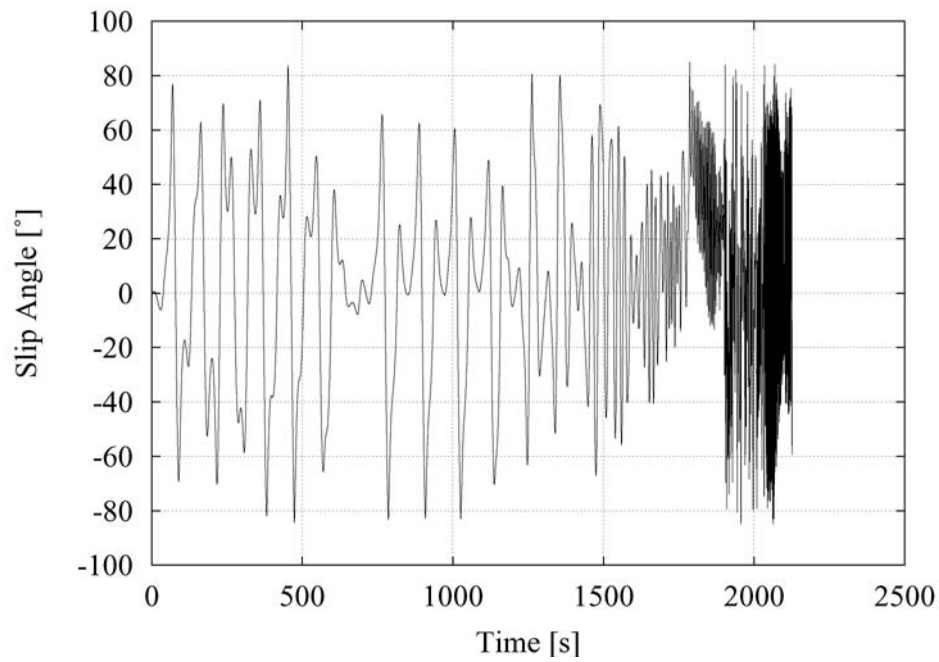


Figure 3-6: Slip Angle History of the Main Object

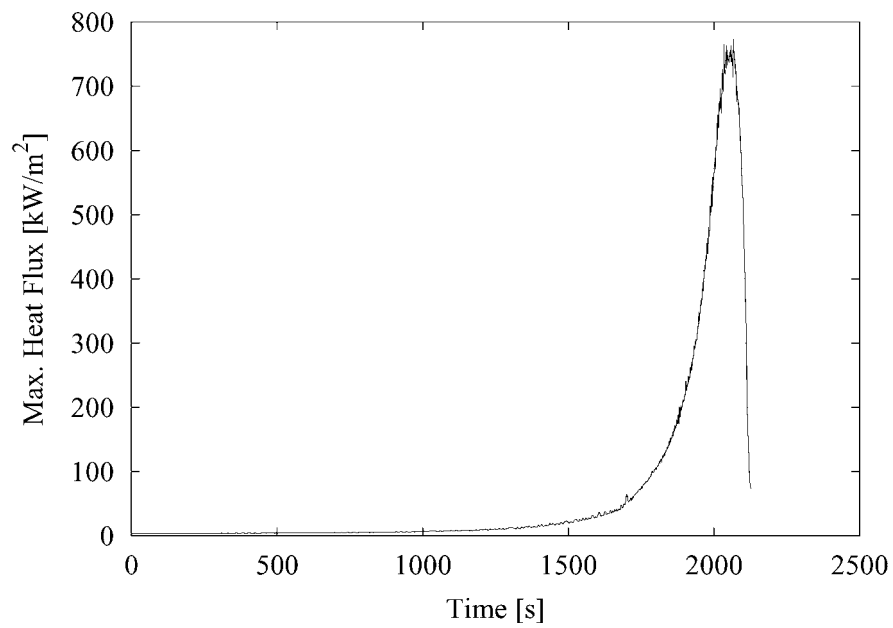


Figure 3-7: Maximum Heat Flux History of the Main Object

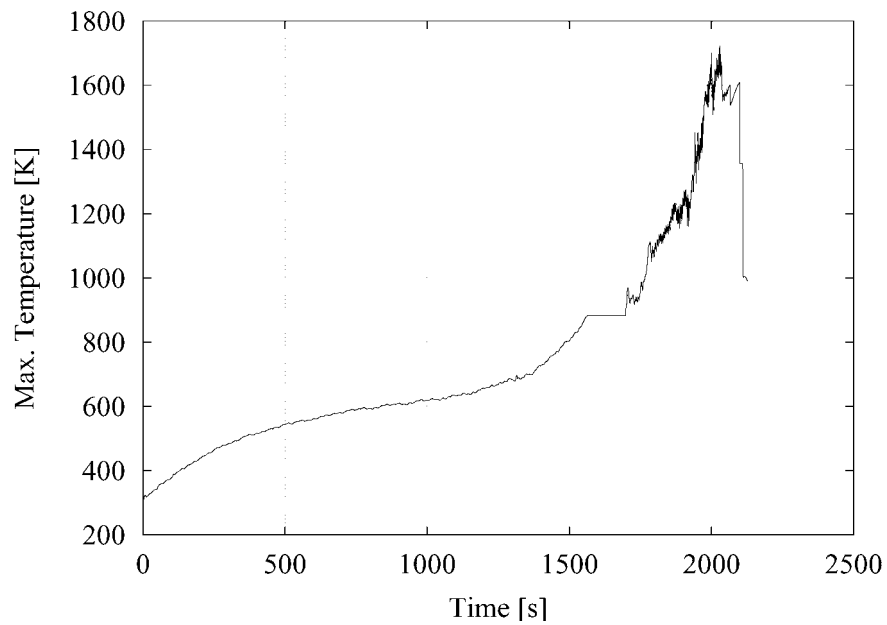


Figure 3-8: Maximum Temperature History of the Main Object

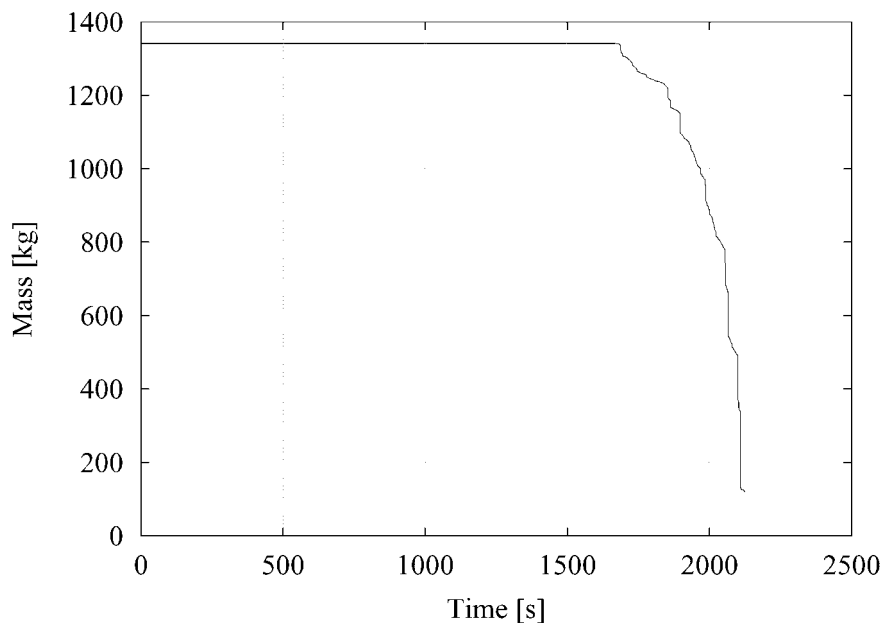


Figure 3-9: Mass History of the Main Object

The fragmentation history describes all fragmentation events during the re-entry. Each fragment is tracked until it either fragmentizes again, demises, or reaches the ground. Figure 3-10 shows the distribution of all the events along the main trajectory (trajectory of the main object). Table 3-3 summarizes all events during the re-entry. It includes the number of each event type and the time and altitude range in which they have occurred.

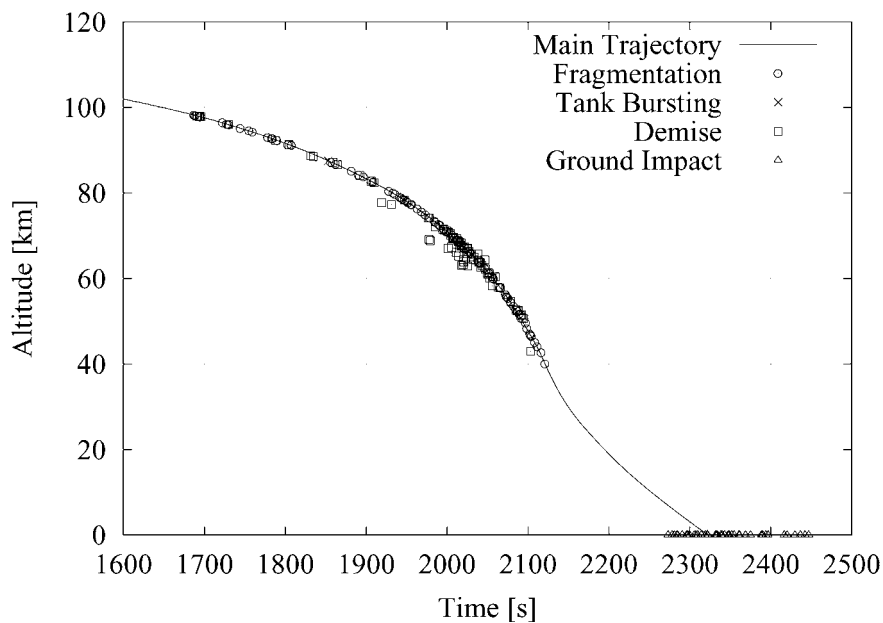


Figure 3-10: BeppoSAX Event Distribution along the Main Trajectory

EVENTS DURING RE-ENTRY			
Event	No.	Time range [s]	Altitude range [km]
Fragmentation	85	1687 – 2121	98.2 – 40.0
Tank bursting	1	1853	87.5
Demise	87	1690 – 2103	98.0 – 43.0
Ground impact	42	2273 – 2447	0.0
Total	215	–	–

Table 3-3: Events during Re-entry

It can be seen that the ranges both for time and for altitude are almost the same. Shortly after the first fragmentation event also the first demise event occurs, because at the beginning of the re-entry only small fragments are generated. Demise stops some seconds before and some kilometers above the last fragmentation event. The last generated fragments reach ground without further fragmentation.

The fragmentation altitude range covers about 49% of the altitude range of the complete re-entry. This shows the important influence of shielding effects on exposure time and altitude for internal parts of the spacecraft.

3.3 Ground Impact Fragments

Table 3-4 gives an overview for the 42 fragments reaching the ground. Each fragment is specified by a number, its name, mass, and mean cross-section area. Images of these fragments are shown in Figure 3-11.

Altogether, 42 fragments of BeppoSAX reach ground with a total mass of 656.226 kg. This corresponds to 48.92% of the initial mass at the beginning of the calculation (1,341.485 kg). The small difference of 43.934 kg (3.17%) between the total mass at the beginning of the calculation and the total model mass results from the panelizing of the geometry.

The fragment dispersion on ground is shown in Figure 3-12. All the fragments are spread out over an area of about 10,500 km² (315.3 x 33.3 km). The impacts take place close to the ground track of the main object.

The impact velocities vary between 16.9 and 128.6 m/s respectively 60.9 and 462.8 km/h. Figure 3-13 shows the impact velocities of the fragments vs. their mass to area ratio. It is shown that the impact velocity of a fragment corresponds with its aerodynamic free fall velocity. Analytic solutions for constant drag coefficients C_D between 0.3 and 0.6 are also shown. The fragments impact on the ground vertically.



GROUND IMPACT FRAGMENTS				
No.	Fragment	Material	Mass [kg]	MCSA ¹ [m²]
1	Solar panel bracket	A316	0,204	0,003
2	Battery	AA7075	14,927	0,083
3	Scientific payload: HP-GSPC	AA7075 TiAl6V4	71,683	0,250
4	HP-GSPC support structure	TiAl6V4	0,699	0,014
5	Power Distribution Unit	AA7075	6,270	0,084
6	Tank	TiAl6V4	5,524	0,160
7	Power Protection & Distribution Unit	AA7075	5,774	0,084
8	Thermal Control Unit	AA7075	29,861	0,183
9	Pipe segment	TiAl6V4	0,116	0,013
10	Pipe segment	TiAl6V4	0,099	0,014
11	Pipe segment	TiAl6V4	0,118	0,012
12	Pipe segment	TiAl6V4	0,086	0,012
13	Pipe segment	TiAl6V4	0,065	0,012
14	Thrusters with pipe	Inconel 718 TiAl6V4	0,720	0,017
15	Thrusters with pipe	Inconel 718 TiAl6V4	0,704	0,018
16	Harness	Copper	2,735	0,019
17	Harness	Copper	3,060	0,019
18	Harness	Copper	8,792	0,047
19	Dummy/balance mass	AA7075	11,135	0,071
20	Dummy/balance mass	AA7075	11,342	0,029
21	Support structure	AA7075	0,004	0,000
22	Tape Recorder Unit	AA7075	5,648	0,038
23	Thrusters block with pipe	Inconel 718 TiAl6V4	1,395	0,026
24	HP-GSPC support structure	TiAl6V4	0,420	0,007
25	HP-GSPC support structure	TiAl6V4	0,420	0,007
26	Thrusters block with pipe	Inconel 718 TiAl6V4	1,357	0,026
27	Scientific payload: LECS/MECS	CFRP TiAl6V4 A316 Invar Copper AA7075	59,721	0,480
28	Scientific payload: LECS/MECS	CFRP TiAl6V4 A316 Invar Copper AA7075	60,449	0,481
29	Support structure	AA7075	0,008	0,000
30	Support structure	AA7075	0,009	0,000
31	Reaction wheel, payload electronics (HP-GSPCE)	HC-AA5052-50mm A316 AA7075	14,607	0,146
32	Reaction wheel	A316 AA7075	5,579	0,046
33	Thrust Cone (structure)	AA2024	12,508	0,336
34	Scientific payload: PDS Core	AA7075 Copper TiAl6V4	92,779	0,221

¹ Mean Cross-Section Area



No.	Fragment	Material	Mass [kg]	MCSA [m²]
35	Scientific payload: PDS Shield	AA7075 TiAl6V4	72,138	0,253
36	Support structure	HC-AA5052-50mm HC-AA5052-C-30mm	0,371	0,033
37	Magnetic torquers	Copper	1,788	0,018
38	WFC support structure	TiAl6V4 AA7075	2,399	0,018
39	Reaction wheel, gyroscope electronics	HC-AA5052-20mm HC-AA5052-50mm AA7075 A316	10,573	0,146
40	Reaction wheel, payload electronics (MEE)	HC-AA5052-50mm AA7075 A316	15,956	0,149
41	Main Object	HC-AA5052-20mm HC-AA5052-50mm HC-AA5052-C-20mm HC-AA5052-C-30mm AA7075 TiAl6V4 Copper	119,877	0,868
42	Main Bus Unit	HC-AA5052-20mm AA7075	4,306	0,036

Table 3-4: Ground Impact Fragments

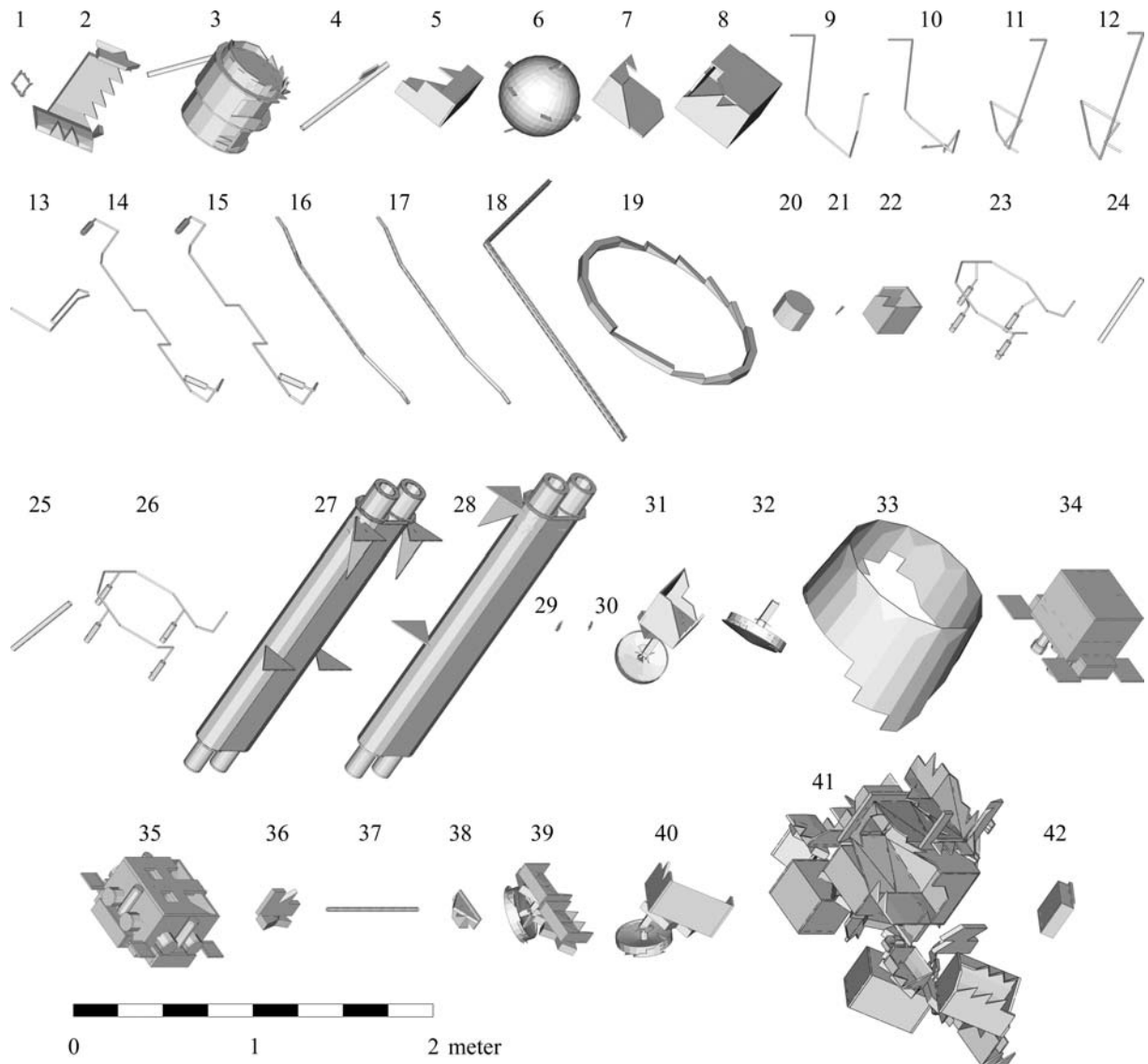


Figure 3-11: Ground Impact Fragments of BeppoSAX



GROUND IMPACT DISTRIBUTION				
No.	Longitude [°]	Latitude [°]	Velocity [m/s]	Kinetic Energy [J]
1	-117.096	2.478	65.69	440.1
2	-114.762	2.339	71.10	37733.0
3	-114.492	2.309	108.32	420544.1
4	-115.011	2.337	43.50	661.4
5	-115.290	2.351	48.61	7406.7
6	-115.550	2.364	41.71	4806.2
7	-115.231	2.331	45.18	5894.1
8	-114.866	2.324	74.44	82733.2
9	-116.066	2.392	19.35	21.7
10	-116.127	2.410	16.96	14.2
11	-116.066	2.395	19.66	22.8
12	-116.158	2.404	16.93	12.3
13	-116.161	2.412	17.66	10.1
14	-115.518	2.362	37.25	499.5
15	-115.454	2.395	35.95	455.0
16	-114.500	2.522	81.68	9123.7
17	-114.552	2.565	84.87	11020.5
18	-114.647	2.365	72.66	23206.9
19	-114.793	2.454	65.97	24227.0
20	-114.230	2.385	128.57	93735.7
21	-115.691	2.378	37.03	2.7
22	-114.867	2.323	79.23	17725.2
23	-115.395	2.349	47.68	1585.5
24	-115.507	2.362	56.10	660.9
25	-115.434	2.361	56.44	669.1
26	-115.349	2.353	44.31	1331.9
27	-114.825	2.331	59.10	104306.2
28	-114.806	2.314	59.38	106554.6
29	-115.630	2.374	38.74	6.0
30	-115.639	2.371	38.88	6.8
31	-114.836	2.332	61.96	28035.1
32	-114.794	2.326	59.32	9815.4
33	-115.103	2.348	34.95	7638.7
34	-114.402	2.294	116.68	631540.7
35	-114.510	2.304	100.84	366806.3
36	-115.349	2.374	18.98	66.8
37	-114.743	2.305	70.92	4497.0
38	-114.740	2.332	65.60	5161.4
39	-114.894	2.339	52.64	14646.0
40	-114.839	2.339	65.41	34129.2
41	-114.855	2.288	68.32	279733.4
42	-114.938	2.262	60.00	7749.5

Table 3-5: Ground Impact Distribution

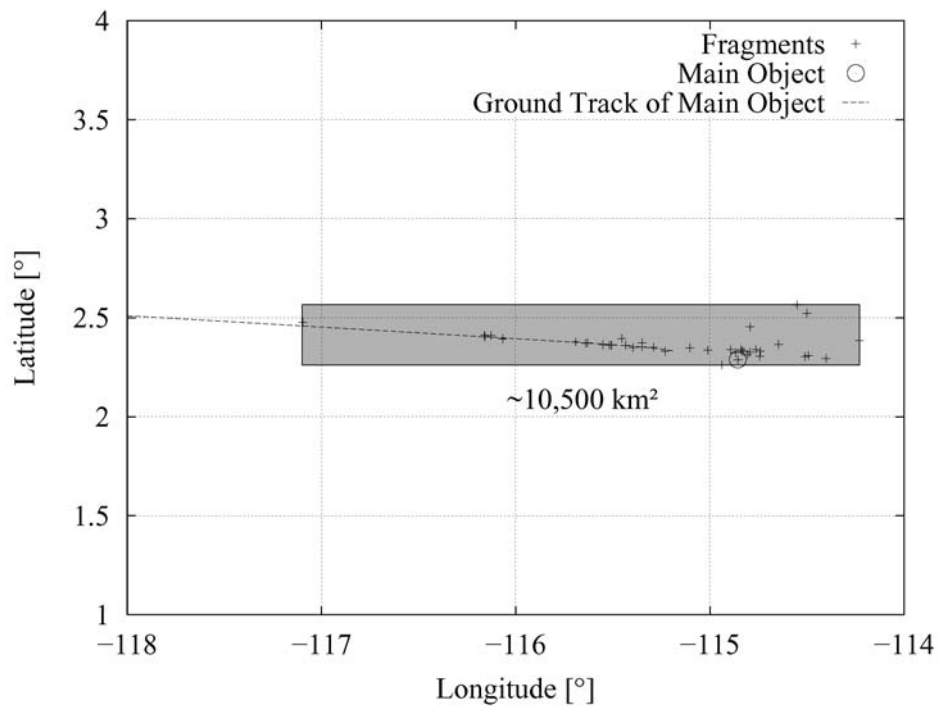


Figure 3-12: Ground Dispersion of Fragments

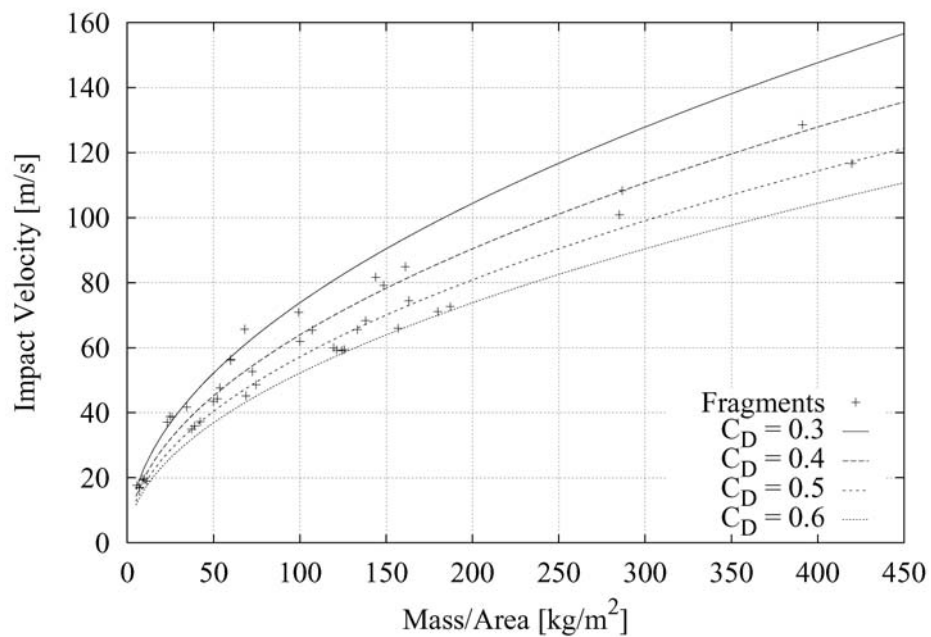


Figure 3-13: Impact Velocities of Fragments

3.4 Casualty Area

The casualty area D_A has been defined by NASA [5]. It indicates the ground risk for human casualties and is calculated as follows:

$$D_A = \sum_i (0,6 + \sqrt{A_i})^2 \quad (\text{Eq. 5-1})$$

where A_i is the cross-section area of each fragment in square meters.

The NASA Safety Standard [5] requires that the casualty area for an uncontrolled re-entry shall not exceed 8 m².

The casualty area for all the ground impact fragments listed in Table 3-4 is calculated to

$$32.419 \text{ m}^2$$

The mass distribution histogram in Figure 3-14 and the diagram of the casualty area of the fragments vs. mass in Figure 3-15 show that most of the fragments (36) are heavier than 0.1 kg. But even the smallest fragments would contribute minimum 0.36 m² to the total casualty area although they would not harm people in the case of a casualty.

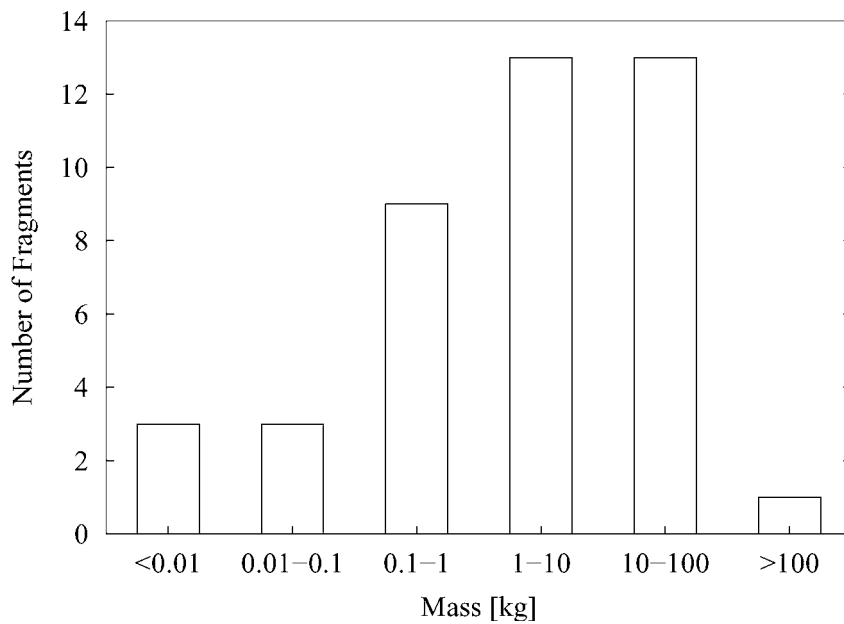


Figure 3-14: Mass Distribution Histogram

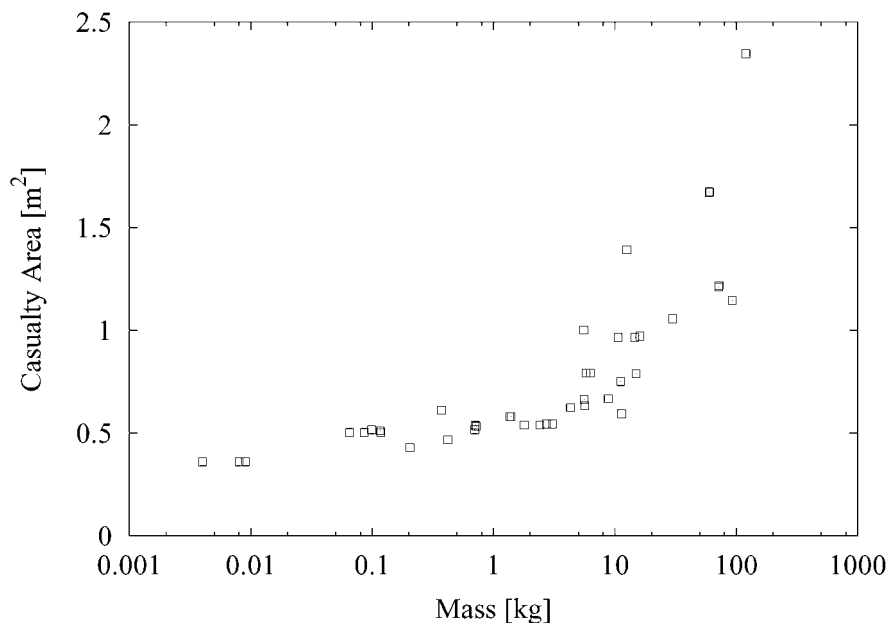


Figure 3-15: Casualty Area of Fragments vs. Mass

Cole et al. [6] have analyzed the probability of fatality from debris impacts on the human body averaged for different body parts (head, thorax, abdomen & limbs) and body positions (standing, sitting, prone) with respect to the kinetic energy of the impacting fragments. With a mean probability of fatality (50%) for 103 J (76 ft-lbf) the kinetic energy limits for 1% and 99% fatality can be calculated to 29 J and 359 J. Figure 3-16 shows the impact velocity vs. the mass of the fragments. Also included in this figure are two lines indicating the 1% and the 99% limit for the probability of fatality.

Figure 3-16 shows that even the fragments smaller than 0.2 kg have probabilities of fatality below 1%.

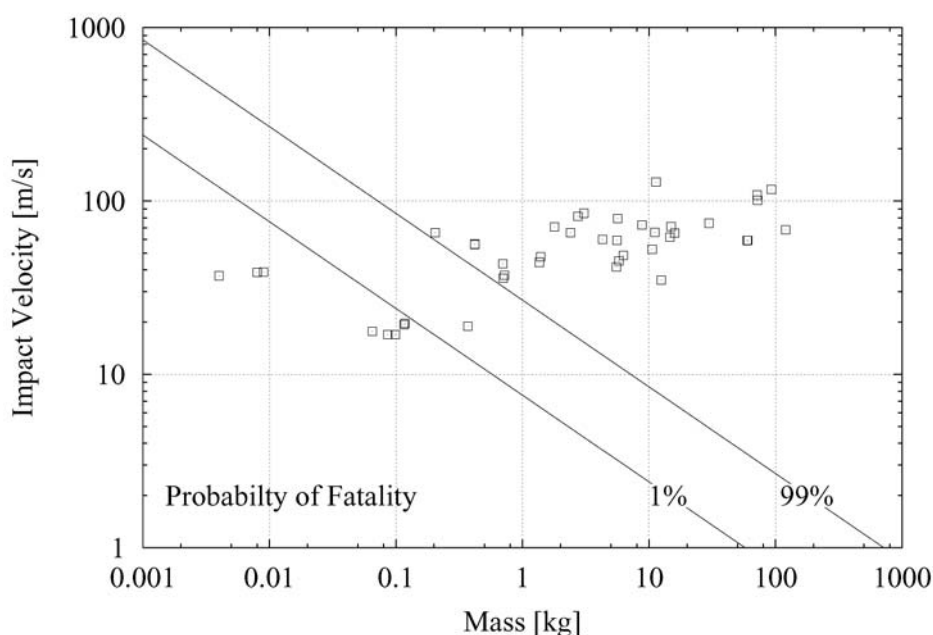


Figure 3-16: Impact Velocity vs. Mass and Probability of Fatality



The threshold for any injury at all is given by Cole et al. [6] with 14.9 J (11 ft-lbf). All fragments smaller than 0.1 kg are below this threshold.

If fragments smaller than 0.1 kg (0.2 kg) are neglected the casualty area is calculated to 29.816 m² (28.803 m²).

4 SUMMARY

In summary, it can be said that a very high and accurate level of modeling has been achieved for BeppoSAX. Primarily the mass and mass distribution of the model corresponds almost completely to the data of the real satellite. The model mass difference is below 0.02%, the center of gravity location of the complete BeppoSAX model matches the actual center of gravity within 11 mm, and the modeled moments of inertia agree within the following bands: $I_{xx} < 3.3\%$, $I_{yy} < 0.9\%$, $I_{zz} < 5.8\%$.

Due to the high complexity of the geometry and due to the asymmetric shape of the satellite, the modeling effort was also higher than expected. This results in the very complex model with 859 primitives and about 178.000 surface panels.

The following comparison with SCARAB models for other satellites/spacecrafts, which HTG treated in the early past, reveals that this is the most complex model:

- Ariane EPC: 200 primitives, 94.000 surface panels
- Ariane EPS/VEB: 229 primitives, 65.000 surface panels
- ATV: 311 primitives, 95.000 surface panels
- ROSAT: 272 primitives, 123.000 surface panels
- BeppoSAX: 809 primitives, 178.000 surface panels

Due to the resulting model complexity also the effort for the destructive re-entry analysis has been increased. Together this analysis yields 2.9 GB data. The complete analysis has taken about 3 weeks (~3 Pentium III processors at 1.2 GHz).

Altogether, 42 fragments reach ground with a total mass of 656.226 kg. This corresponds to 48.92 % of the initial mass at the beginning of the calculation (1341.485 kg).

The ground impact fragments have been analyzed and the ground risk has been determined by using the NASA casualty area. The casualty area for all the fragments has been calculated to 32.419 m². If fragments with a mass below 0.1 kg (0.2 kg) are neglected the casualty area is calculated to 29.816 m² (28.803 m²).

REFERENCES

- [1] Lips, T., *SCARAB Model for BeppoSAX*, Technical Note, HTG-TN-02-5, HTG – Hyperschall Technologie Göttingen, Katlenburg-Lindau, Germany, 2002.
- [2] Lips, T., *BeppoSAX Re-entry Analysis*, Technical Note, HTG-TN-02-8, HTG – Hyperschall Technologie Göttingen, Katlenburg-Lindau, Germany, 2002.
- [3] Fritsche, B., G. Koppenwallner, T. Roberts, et al., *Spacecraft Disintegration during Atmospheric Re-entry*, Executive Summary, ESOC Contract No. 11427/95/D/IM, HTG-Report-97-6, HTG – Hyperschall Technologie Göttingen, Katlenburg-Lindau, Germany, 1997.
- [4] Fritsche, B., G. Koppenwallner, M. Ivanov, et al., *Advanced Model for Spacecraft Disintegration during Atmospheric Re-entry*, Executive Summary, ESOC Contract No. 12804/98/D/IM, HTG-Report-00-4, HTG – Hyperschall Technologie Göttingen, Katlenburg-Lindau, Germany, 2000.
- [5] Anonym, *NASA Safety Standard – Guidelines and Assessment Procedures for Limiting Orbital Debris*, NSS 1740.14, NASA, Office of Safety and Mission Assurance, Washington D.C., 1995.
- [6] Cole, J. Kenneth, Larry W. Young, Terry Jordan-Culler, *Hazards of Falling Debris to People, Aircraft, and Watercraft*, Sandia Report, SAND97-0805 – UC-706, Sandia National Laboratories, Albuquerque, USA, 1997.

BeppoSAX Documents:

- [7] SAX Satellite Mass Budget Report (SX-RP-AI-003), Issue 12, 30/06/94
- [8] SAX System Design Report (SX-RP-AI-118), Issue 01, 10/01/94
- [9] Mass Properties Status Report Structure (SX-RP-AI-0031), Issue 06, 19/07/94